CONF-941144--98

Note: This is a preprint of a paper being submitted for publication. Contents of this document should not be quoted or referred to without permission of the author(s).

To be submitted to Fall 1994 Materials Research Society Meeting, Symposium F: Microcrystalline and Nanocrystalline Semiconductors, ed. by L. Brus, R. W. Collins, M. Hirose, F. Koch, and C. C. Tsai.

Semiconductor Nanocrystals Formed in SiO_2 by Ion Implantation

Jane G. Zhu, C. W. White, J. D. Budai,
S. P. Withrow, and Y. Chen

Oak Ridge National Laboratory
Bldg. 3137, P.O. Box 2008
Oak Ridge, TN 37831-6057

SOLID STATE DIVISION
OAK RIDGE NATIONAL LABORATORY
Managed by
MARTIN MARIETTA ENERGY SYSTEMS, INC.
under
Contract No. DE-AC05-84OR21400
with the
U. S. DEPARTMENT OF ENERGY

November 1994

DISCLAIMER

SEMICONDUCTOR NANOCRYSTALS FORMED IN SiO_2 BY ION IMPLANTATION

JANE G. ZHU, C. W. WHITE, J. D. BUDAI, S. P. WITHROW, AND Y. CHEN*
Oak Ridge National Laboratory, Solid State Division, P.O. Box 2008, Oak Ridge, TN 37831

ABSTRACT

Nanocrystals of group IV (Si, Ge and SiGe), III-V (GaAs), and II-VI (CdSe) semiconductor materials have been fabricated inside SiO_2 by ion implantation and subsequent thermal annealing. The microstructure of these nanocrystalline semiconductor materials has been studied by transmission electron microscopy (TEM). The nanocrystals form in near-spherical shape with random crystal orientations in amorphous SiO_2. Extensive studies on the nanocrystal size distributions have been carried out for the Ge nanocrystals by changing the implantation doses and the annealing temperatures. Remarkable roughening of the nanocrystals occurs when the annealing temperature is raised over the melting temperature of the implanted semiconductor material. Strong red photoluminescence peaked around 1.67 eV has been achieved in samples with Si nanocrystals in SiO_2.

INTRODUCTION

Semiconductor nanocrystals, also termed quantum dots, are attractive materials due to their potential applications in optoelectronics. Quantum confinement effects and surface or interface states are considered to be the dominant factors for the visible photoluminescence (PL) of group IV semiconductor nanocrystallites [1-4]. Finite-size effects also substantially enhance the optical nonlinearity of II-VI nanocrystals [5-7]. To obtain three-dimensionally confined systems, many groups have exploited a variety of techniques, for example, pyrolysis for nanocrystal colloids [3,8], wet micromilling of bulk material [9], cosputtering [10-12], pulsed laser ablation [13], chemical vapor deposition [14] and ion implantation [4, 15-16].

The ion implantation technique has been utilized in our study. This technique can produce a controlled depth distribution of desired species and is extensively used in semiconductor technology. This paper presents a study of Ge, Si, SiGe, GaAs and CdSe nanocrystals in thermally grown SiO_2, with emphasis on Ge. Thermally grown SiO_2 on Si wafers is not only a stable matrix for the nanocrystals, but also well characterized and suited for semiconductor processing. Cross-sectional transmission electron microscopy (TEM) is extensively used to investigate the nanocrystal formation at various conditions. PL measurements are used to characterize the optical properties. Related results on semiconductor nanocrystals in other matrices can be found elsewhere [17].

EXPERIMENTAL

The semiconductor nanocrystals were formed by ion implantation (at room temperature) of semiconductor species into a SiO_2 layer on (100) silicon substrate and subsequent thermal

*Present address: U.S. Department of Energy, ER 131, Division of Materials Sciences, Washington D.C. 20585

annealing. A typical SiO_2 layer was 750 nm thick, formed by thermally oxidizing a (100) Si wafer. The implanted species included Ge, Si, Si+Ge, Ga+As, and Cd+Se, with doses of (0.6 to 3)$\times 10^{17}$ ions/cm^2. Implant energies were chosen to put the peak concentration at the center of the oxide layer. For the compound semiconductors, equal doses of each constituent were implanted. Samples were annealed isochronally for 1 hr under $Ar + 4\%H_2$ ambient. The annealing temperatures varied from 600°C to 1100°C.

The nanocrystalline structures were investigated by TEM and X-ray diffraction. All the TEM specimens were prepared in cross sections, since the concentration distribution from ion implantation is a function of depth. Depth profiles were also examined by Rutherford backscattering spectrometry. PL and Raman spectra were measured at room temperature using an Ar-ion laser as the excitation source.

RESULTS AND DISCUSSION

A series of samples have been implanted with different doses of Ge (400 keV) into SiO_2 and annealed at different temperatures to study the effects of dose and annealing temperature on the nanocrystal formation. The cross-sectional TEM pictures of three samples are shown in Fig. 1. The Ge particles are spherical in shape, as is expected for an amorphous matrix. A wide range of particle sizes, from 1 to 25 nm, is observed in the sample implanted with 3×10^{17} ions/cm^2 and annealed at 1000°C (Fig. 1a). At the peak of the concentration profile, the largest crystallites are ~ 25 nm in diameter. The peak of the size distribution profile over the whole implanted region is at ~ 5 nm (Fig. 1d). It is worthy to point out that plan-view TEM may provide only part of the picture when the nanocrystal size is a function of depth. In some large precipitates, crystal defects, such as twinning, have been observed. The nanocrystallites are randomly oriented.

As the dose of the implanted Ge decreases, the high end of the size distribution reduces rapidly. In a sample implanted with 1.5×10^{17} ions/cm^2 and annealed at 1000°C (not shown), the sizes of Ge nanocrystals range from 1 to 12 nm. At an even lower dose of 6×10^{16}/cm^2, the Ge nanocrystal sizes are all smaller than 7 nm, with the peak of the size distribution profile at ~ 4.5 nm (Fig. 1b and 1e). It is noticed that in a sample where the size distribution covers a large size range, there is a higher number density of small nanocrystals closer to the surface (upper side of the implanted region, see Fig. 1a). This phenomenon is much less visible in samples with narrower size distributions.

Another controlling factor for the size distribution is the annealing temperature. The sample implanted with a high dose of 3×10^{17}/cm^2, but annealed at a low temperature of 600°C, contains Ge nanocrystals with sizes between 1 nm to 9 nm (Fig. 1c and 1f). The sizes of the majority of the nanocrystals are smaller than 5 nm, and the peak of the size distribution profile is at ~ 4 nm. Although the samples shown in Figs. 1(b) and 1(c) contain smaller sizes of nanocrystals, the sample implanted with a high dose but annealed at a low temperature (Fig. 1c) has a much higher number density of nanocrystals than that implanted with a low dose but annealed at a high temperature (Fig. 1b). In samples implanted with the high dose, no substantial change in nanocrystal sizes has been observed when annealed at 800°C compared with the sample annealed at 600°C. When the annealing temperature is increased to 1000°C, a dramatic increase in sizes appears for the nanocrystals located at the peak area of the concentration depth profile, where there is more Ge for large particles to grow. Small nanocrystals are usually desired in order to excite efficient photoluminescence.

Under similar processing conditions, the Si (implanted at 400 keV) nanocrystals formed in SiO_2 are much smaller. A cross-sectional high resolution electron microscopy (HREM) image of a

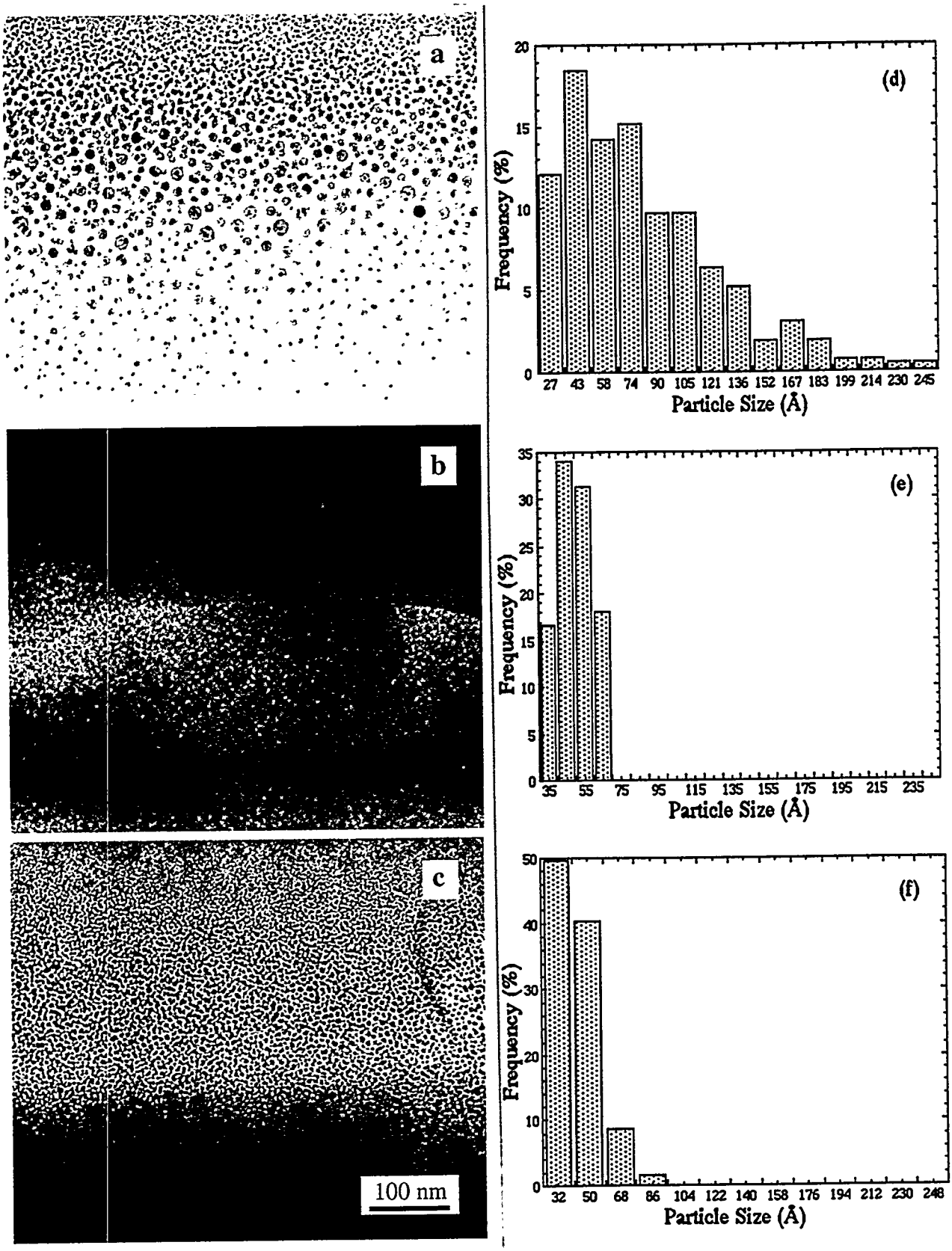

Fig. 1. Cross-sectional TEM images of samples with Ge doses and annealing temperatures of (a) $3\times10^{17}/cm^2$, 1000°C/1 hr, (b) $6\times10^{16}/cm^2$, 1000°C/1 hr, and (c) $3\times10^{17}/cm^2$, 600°C/1 hr. Corresponding Ge nanocrystal size distributions of samples a, b and c are in (d), (e) and (f), respectively.

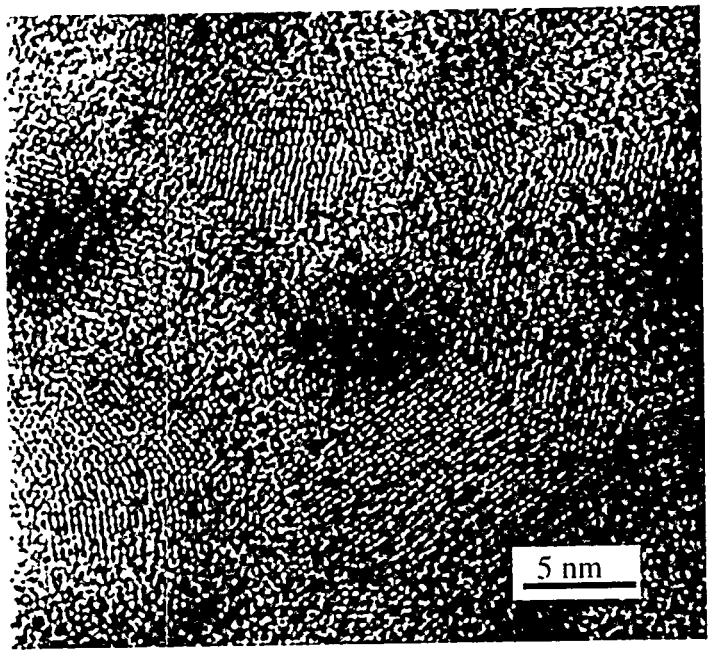

Fig. 2. Cross-sectional HREM image of Si nanocrystals in a sample implanted with 6×10^{17}ions/cm^2 and annealed at 1100°C for 1 hr.

Si-implanted sample with a dose of 6×10^{17}/cm^2 and annealed at 1100°C is shown in Fig. 2. The Si nanocrystals are smaller than 6 nm, with a high number density. Compared to the samples with Ge nanocrystals in Fig. 1(a), this sample has a higher dose and has been annealed at a higher temperature, but contains much smaller nanocrystals. In the sample implanted with a dose of 3×10^{17}/cm^2 and annealed at 1000°C, the sizes of the Si nanocrystals are even smaller, ~ 3 nm.

The remarkable difference in sizes of the Ge and Si nanocrystals indicates that there is no rapid increase in crystallite size until the annealing temperature approaches the melting temperature of the implanted material. The annealing temperature (1000°C) for the Ge-nanocrystal sample shown in Fig. 1(a) is above the melting temperature of Ge (938.3°C), while the annealing temperature (1100°C) for the Si-nanocrystal sample shown in Fig. 2 is well below the melting temperature of Si (1414°C). To demonstrate the enormous size increase of the precipitates at the melting temperature, a sample was implanted with Si (215 keV, 3×10^{17}/cm^2) and Ge (500 keV, 3×10^{17}/cm^2) sequentially and post annealed at ~ 1100°C, near the melting point of the alloy. As shown in Fig. 3, very large SiGe precipitates are formed at the center region, including particles with dimensions greater than 100 nm. Besides coarsening, some precipitates have coalesced. The smaller particles along the edges of the implanted region are still in near-spherical shape. In the SiGe alloy system, imperfect overlap of implantation profiles or a mix of melted and solid material during annealing generates non-uniform composition, which undesirably complicates the system. When a sample with the same high dose of SiGe is annealed at 1000°C (lower than the melting point of the alloy), the largest precipitates are smaller than 15 nm, and spherical in shape.

Other compound semiconductor nanocrystals formed in SiO_2 include GaAs and CdSe nanocrystals. Figure 4 shows HREM images from samples containing (a) equal dose (1.5×10^{17}/cm^2) of Ga (470 keV) and As (500 keV) and annealed at 1000°C, and (b) equal dose (1×10^{17}/cm^2) of Cd (450 keV) and Se (330 keV) and

Fig. 3. SiGe precipitates in SiO_2 after annealed at ~ 1100°C for 1 hr.

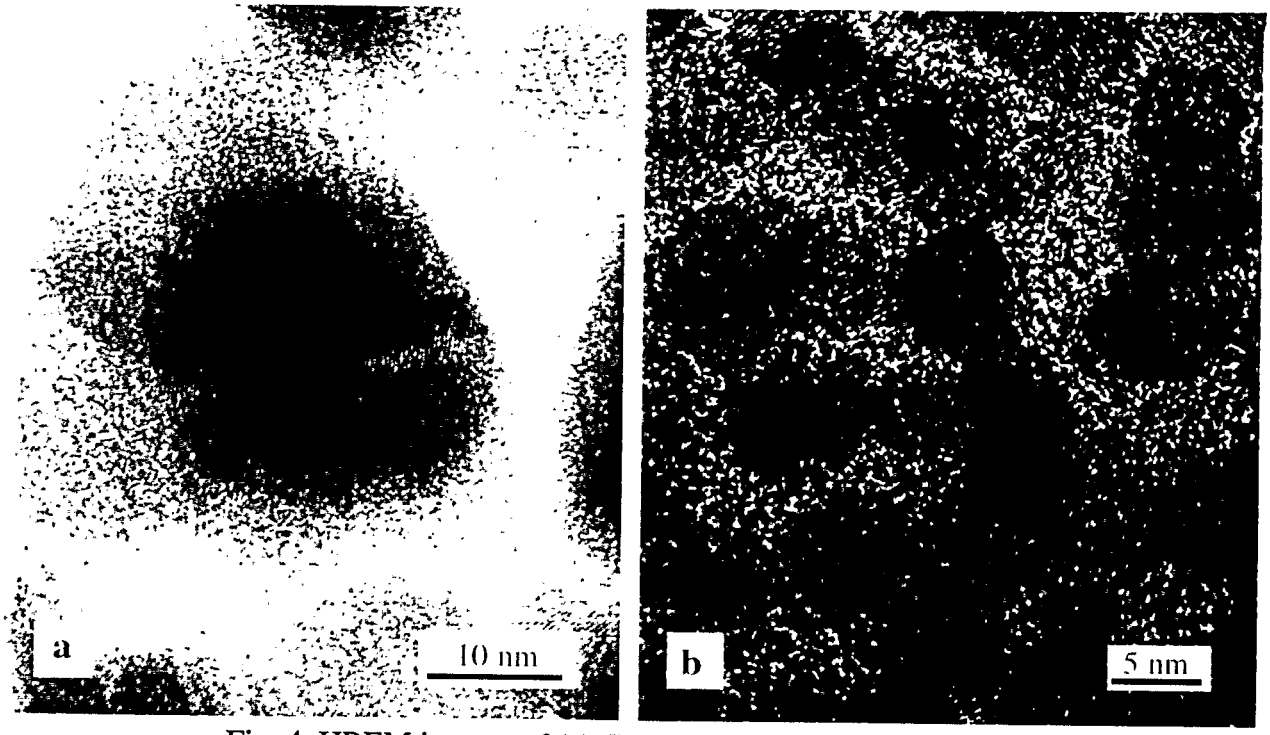

Fig. 4. HREM images of (a) GaAs and (b) CdSe nanocrystals.

annealed at 1000°C. Similar to the Ge nanocrystals, large GaAs nanocrystals contain crystal defects such as twinning (Fig. 4a). Such defects could affect the optical properties. Both the GaAs and CdSe nanocrystals are nearly spherical. X-ray diffraction shows that the CdSe has the hexagonal wurtzite structure. The size distributions of the nanocrystals depend on the doses and annealing temperatures as discussed above. Further investigation on the formation of compound semiconductor nanocrystals is in progress.

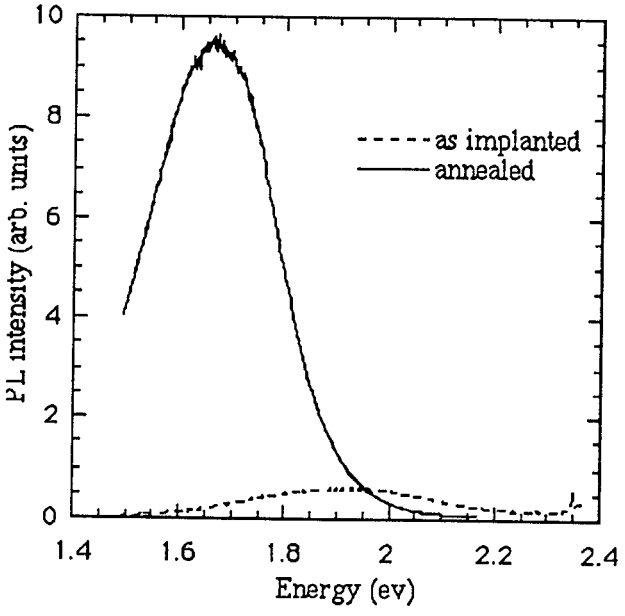

Fig. 5. PL spectra of Si^+ implanted SiO_2 to a dose of 6×10^{17}ions/cm^2 and annealed at 1100°C for 1 hr.

Among these semiconductor-nanocrystal-containing samples, the strongest PL intensity is detected in the Si^+-implanted samples with high doses and annealed at 1100°C. The sample implanted with a high Si dose of 6×10^{17}/cm^2 contains a large number of small nanocrystals (1-6 nm) as shown in Fig. 2. The PL spectra from this sample, shown in Fig. 5, are measured at room temperature and excited by 50 mW of 514 nm radiation from an Ar ion laser. The PL spectrum from the as-implanted sample has a broad peak around 1.95 eV. After thermal annealing at 1100°C, the PL peak red shifts to 1.67 eV with an intensity 15 times the peak intensity from the as implanted sample. The peak position shift upon annealing is in agreement with the previously reported work [4]. However, the PL intensity from the annealed sample presented here is much stronger in reference to the PL from the as-implanted

sample. The PL intensity is sensitive to the Si doses, annealing temperature and annealing ambient. Detailed PL results will be published elsewhere.

CONCLUSIONS

Semiconductor nanocrystals of Ge, Si, SiGe, GaAs and CdSe have been formed in SiO_2, which is thermally grown on Si wafers, by ion implantation and subsequent thermal annealing. Effects of dose and temperature have been investigated in depth for the Ge nanocrystals. Lower doses tend to produce smaller nanocrystals. Roughening of the nanocrystals is significant when the annealing temperature is above the melting temperature. The effect of annealing temperature on nanocrystal sizes is also demonstrated in the Si and SiGe nanocrystal systems. All the elemental and compound semiconductor nanocrystals are in spherical shape with random crystal orientation in amorphous SiO_2. Twinning defects are observed in the large nanocrystals, which could affect the optical properties. Strong PL peaked 1.67 eV is observed in Si-nanocrystal-containing samples. The PL intensity is more than an order of magnitude higher than that of the broad peak around 1.95 eV from the as implanted sample.

ACKNOWLEDGMENT

This research was sponsored by the Division of Materials Sciences, U.S. Department of Energy, under contract DE-AC05-84OR21400 with Martin Marietta Energy Systems, Inc., and supported in part through the ORNL Postdoctoral Research Program administered by ORISE.

References

1. L. T. Canham, Appl. Phys. Lett. **57**, 1046 (1990).
2. W. L. Wilson, P. F. Szajowski, and L. E. Brus, Science **262**, 1242 (1993).
3. K. A. Littau, P. J. Szajowski, A. J. Miller, A. R. Kortan, and L. E. Brus, J. Phys. Chem. **97**, 1224 (1993).
4. T. Shimizu-Iwayama, K. Fujita, S. Nakao, K. Saitoh, T. Fujita, and N. Itoh, J. Appl. Phys. **75**, 7779 (1994).
5. R. K. Jain and R. C. Lind, J. Opt. Soc. Am. **73**, 647 (1983).
6. E. Hanamura, Phys. Rev. B **37**, 1273 (1988).
7. L. Brus, Appl. Phys. A **53**, 465 (1991).
8. C. B. Murry, D. J. Norris, and M. G. Bawendi, J. Am. Chem. Soc. **115**, 8706 (1993), and the references therein.
9. S. Juen, K. Überbacher, J. Baldauf, K. F. Lamprecht, R. Tessadri, R. Lackner, R. A. Höpfel, Superlattices and Microstructures **11**, 181 (1992).
10. Y. Maeda, N. Tsukamoto, Y. Yazawa, Y. Kanemitsu, and Y. Masumoto, Appl. Phys. Lett. **59**, 3168 (1991).
11. Y. Osaka, K. Tsunetomo, F. Toyomura, H. Myoren, and K. Kohno, Jpn. J. Appl. Phys. **31**, L365 (1992).
12. S. Hayashi, T. Nagareda, Y. Kanzawa, and K. Yamamoto, Jpn. J. Appl. Phys. **31**, 3840 (1993).
13. E. Werwa, A. A. Seraphin, L. A. Chiu, C. Zhou, and K. D. Kolenbrander, Appl. Phys. Lett. **64**, 1821 (1994).
14. X. Liu, X. Wu. X. Bao, and Y. He, Appl. Phys. Lett. **64**, 220 (1994).
15. H. A. Atwater, K. V. Shcheglov, S. S. Wong, K. J. Vahala, R. C. Flagan, M. L. Brongersma, and A. Polman, Mat. Res. Soc. Symp. Proc. **316**, 409 (1994).
16. C. W. White, J. D. Budai, S. P. Withrow, S. J. Pennycook, D. M. Hembree, D. S. Zhou, T. Vo-Dinh, and R. H. Magruder, Mat. Res. Soc. Symp. Proc. **316**, 487 (1994).
17. C. W. White, J. D. Budai, J. G. Zhu, S. P. Withrow, R. A. Zuhr, Y. Chen, D. M. Hembree, R. H. Magruder, and D. O. Henderson, in this proceedings book.